

Subject: Soils – Geophysical Field Assistance

Date: 20 July 2001

To: Mary K. Combs
State Conservationist
USDA-NRCS,
4405 Bland Road, Suite 205
Raleigh, North Carolina 27609

Purpose:

The purpose of this investigation was to help characterize a Carolina Bay with ground-penetrating radar (GPR) and electromagnetic induction (EMI).

Participants:

Alex Adams, Technician, North Carolina State University, Raleigh, NC
Tripp Cox, Technician, North Carolina State University, Raleigh, NC
Jim Doolittle, Research Soil Scientist, USDA-NRCS, Newtown Square, PA
Justin Ewing, Graduate Student, North Carolina State University, Raleigh, NC
Jared Jenkins, Graduate Student, North Carolina State University, Raleigh, NC
Byron Jenkinson, Research Assistant, Purdue U., Lafayette, IN
Brian Roberts, Technician, North Carolina State University, Raleigh, NC
Jeff White, Assistant Professor, Department of Soil Science, North Carolina State University, Raleigh, NC
Doug Wysocki, Research Soil Scientist, USDA-NRCS, Lincoln, NE
Bill Zanner, Assistant Professor, School of Natural Resource Sciences, University of Nebraska, Lincoln, NE

Activities:

All activities were completed during the period of 11 to 14 June 2001.

Background:

A Carolina Bay will be restored to its original wetland conditions by the North Carolina Department of Transportation. This action is being undertaken to receive wetland credits. Previous wetland restoration efforts have often failed to meet pursued goals. Several interrelated research projects are being carried out at Juniper Bay to ensure that the restoration meets desired objectives. In an earlier investigation (see my trip report of 8 January 2001), the depth and extent of permeable and impermeable layers within the bay were documented with GPR. This study is a continuation of the earlier investigation.

Results:

1. This report summarizes the results of GPR and EMI surveys conducted within Juniper Bay in June 2001. In this report, discussions are principally limited EMI surveys results.

2. A second report will be filed on the three-dimensional images that have been prepared from processed radar profiles. These images appear to provide multiple perspectives from which to view and analyze the subsurface within portions of the bay. The subsurface stratigraphy and geometry of the bay can be interpreted in more detail with three-dimensional than with the more widely spaced two-dimensional radar profiles.
3. All data collected during this investigation have been forwarded to North Carolina State University. A CD containing bitmap files of all radar profiles and a spreadsheet of the EMI data has been forwarded to Jared Jenkins with a copy of this report.

It was my pleasure to work in North Carolina and assist North Carolina State University and members of your staff.

With kind regards,

James A. Doolittle
Research Soil Scientist

cc:

- B. Ahrens, Director, USDA-NRCS, National Soil Survey Center, Federal Building, Room 152,100 Centennial Mall North, Lincoln, NE 68508-3866
- J. Jenkins, Department of Soil Science, North Carolina State University, Box 7619, 3404 Williams Hall, Raleigh, NC 27695.
- Olson, National Leader, Soil Investigation Staff, USDA-NRCS, National Soil Survey Center, Federal Building, Room 152,100 Centennial Mall North, Lincoln, NE 68508-3866
- H. Smith, Director of Soils Survey Division, USDA-NRCS, Room 4250 South Building, 14th & Independence Ave. SW, Washington, DC 20250
- M. Vepraskas, Professor, Department of Soil Science, North Carolina State University, Box 7619, 3404 Williams Hall, Raleigh, NC 27695.
- R. Vick, State Soil Scientist, USDA-NRCS, 4405 Bland Road, Suite 205, Raleigh, North Carolina 27609
- J. White, Assistant Professor, Department of Soil Science, North Carolina State University, Box 7619, 3404 Williams Hall, Raleigh, NC 27695
- W. Zanner, Assistant Professor, School of Natural Resource Sciences University of Nebraska, 133 Keim Hall, Lincoln, NE 68583-0915

Equipment:

The radar unit is the Subsurface Interface Radar (SIR) System-2000, manufactured by Geophysical Survey Systems, Inc.¹ Morey (1974), Doolittle (1987), and Daniels (1996) have discussed the use and operation of GPR. The SIR System-2000 consists of a digital control unit with keypad, VGA video screen, and connector panel. A 12-volt battery powered the system. This unit is backpack portable and, with an antenna, requires two people to operate. A 120 MHz antenna was used in this study. The scanning time was 200 nanoseconds (ns). Hard copies of the radar data were printed in the field on a model GS 608P printer.

Geophysical Survey Systems, Inc manufactures the GEM300 multifrequency sensor.¹ This sensor is portable and requires only one person to operate. No ground contact is required with the GEM300 sensor. This sensor is configured to simultaneously measure up to 16 frequencies between 330 and 19,950 Hz with a fixed coil separation (1.3 m). The GEM300 sensor is keypad operated. Measurements can be either automatically or manually triggered. The theoretical penetration depth of the GEM300 sensor is dependent upon the bulk conductivity of the profiled earthen material(s) and the operating frequency. Multifrequency sounding with the GEM300 allows multiple depths to be profiled with one pass of the sensor.

The location (latitude and longitude) of each EMI observation point was obtained with Rockwell Precision Lightweight GPS Receivers (PLGR).¹ The receiver was operated in the continuous and the mixed satellite modes. The Latitude-Longitude coordinate system was used. Horizontal datum is the North American 1983.

Study Site:

Juniper Bay is an exceeding large Carolina Bay located near Lumberton, Robeson County, North Carolina. The bay is about 1.5 miles long and 1.0 mile wide. The bay has an extensive system of open drainage ditches and covered drain lines. The bay had been planted to cotton last year. This year, the land is idle.

Juniper Bay has been extensively drained for agriculture. Principal soils that have been mapped within Juniper Bay are Leon fine sand, Pantego fine sandy loam, Ponzer muck, and Rutlege loamy sand (McCachren, 1978). The very deep, poorly drained and very poorly drained Leon and the very poorly drained Rutlege soils formed in sandy Coastal Plain sediments. Leon soils are members of the sandy, siliceous, thermic Aeric Alaquods family. Rutlege soils are members of the sandy, siliceous, thermic Typic Humaquepts family. The very deep, very poorly drained Pantego soil formed in medium textured Coastal Plain sediments. Pantego soils are members of the fine-loamy, siliceous, semiactive, thermic Umbric Paleaquults family. The very poorly drained Ponzer soil formed in highly decomposed organic materials that are underlain by medium textured marine and fluvial sediments. Ponzer soils are members of the loamy, mixed, dysic, thermic Terric Haplosaprists family.

Field Procedures:

Surveys were concentrated in the northwestern portion of the bay and in selected areas along the rim and outside the bay. In addition, surveys were completed in eastern areas of the bay that had been selected, but not surveyed because of wet soil conditions during the December 2000 investigation. Lines were of variable lengths. Survey flags were inserted in the ground at intervals of about 30 meter along most traverse line and served as observation points.

Prior to GPR fieldwork, a metallic reflector was buried at a depth of 20 inches and used to estimate the velocity of propagation, dielectric permittivity, and depth scale. The velocity of propagation was estimated to be about 0.08 m/ns in the upper part of the soil profile. Using this velocity of propagation, the maximum depth of observation would be about 7.7 m. However, with increasing soil depths this velocity of propagation will be reduced because of increased soil moisture. In the coarse textured materials below the water table, the velocity is assumed to be 0.05 m/ns.

Pulling the 120 MHz antenna along the traverse lines completed radar surveys. As the radar antenna was pulled passed each observation point, the operator impressed a vertical mark on the radar record. Table 1 summarizes the location, track, and identification of each radar traverse.

¹ Manufacturer's names are provided for specific information; use does not constitute endorsement.

The GEM300 sensor was operated in the station mode. At each observation point, apparent conductivity measurements were taken with the GEM300 sensor held at hip-height (0.9 m) in both the horizontal and vertical dipole orientations. Measurements were obtained at frequencies of 3030, 6090, 9810, and 14790 Hz. At each observation point, inphase, quadrature, and conductivity measurements were obtained at each of the four preset frequencies and with the sensor orientated in both the horizontal and vertical dipole orientation.

File	Core #	Location	Direction	File	Core #	Location	Direction
5	8	center	W to E	42	13		E to W
6	8	edge	E to W	43	13		W to E
7	8	cross	N to S	44	3M		E to W
8	15	center1	E to W	45	3M		E to W
9	15	center2	E to W	46	3K		E to W
10	15	edge2	W to E	47	3K		E to W
11	15	cross	N to S	48	3J		E to W
12	15	edge1	W to E	49	3J		W to E
13	1V		E to W	50	3H		E to W
14	1U		W to E	51	3H		W to E
15	1T		E to W	52	3D		E to W
16	1S		W to E	53	3D		W to E
17	1R		E to W	54	25-1		N to S
18	1Q		W to E	55	25-2		S to N
19	1P		E to W	56	25-3		N to S
20	1O		W to E	57	25-4		S to N
21	1N		E to W	58	25-5		E to W
22	1M		W to E	59	25-6		N to S
23	1L		E to W	60	North Rim		S to N
24	1K		W to E	61	NE Rim		W to E
25	1-S-9		E to W	62	NE Rim		N to S
26	1-S-8		E to W	63	Core 27		W to E
27	1-S-7		E to W	64	Core 27		S to N
28	1-S-6		E to W	65	Core 18		W to E
29	1-S-5		E to W	66	Core 18		N to S
30	1-S-4		E to W	67	Core 24		N to S
31	1-S-3		E to W	68	Core 24		E to W
32	1-S-2		E to W	69	Core 28		N to S
33	1-S-1		E to W	70	Core 28		W to E
34	1-T-8		E to W	71	1J		E to W
35	1-T-7		E to W	72	1I		W to E
36	1-T-6		E to W	73	1H		E to W
37	1-T-5		E to W	74	1G		W to E
38	1-T-4		E to W	75	1F		E to W
39	1-T-3		E to W	76	1D		W to E
40	1-T-2		E to W	77	1C		E to W
41	1-T-1		E to W	78	1B		W to E
				79	1E		E to W

Table 1 – Summary of Radar Records. The sequential file numbers refer to the recorded radar files. The core number identifies the field in which a core was obtained. Location and direction identify the starting position and track of the radar traverse.

Electromagnetic induction uses electromagnetic energy to measure the apparent conductivity of earthen materials. Apparent conductivity is a depth-weighted, average conductivity measurement for a column of earthen materials to a specific depth (Greenhouse and Slaine, 1983). Variations in apparent conductivity are caused by changes in the electrical conductivity of earthen materials. The electrical conductivity of soils is influenced by the type and concentration of ions in solution, the amount and type of clays in the soil matrix, the volumetric water content, and the temperature and phase of the soil water (McNeill, 1980). The apparent conductivity of soils will increase with increased soluble salts, water, and clay contents (Kachanoski et al., 1988; Rhoades et al., 1976).

Interpretations of EMI data are based on the identification of spatial patterns within data sets. Though seldom diagnostic in themselves, lateral and vertical variations in apparent conductivity have been used to infer changes in soils and soil properties. Electromagnetic induction integrates the bulk physical and chemical properties of soils within a defined observation depth into a single value. As a consequence, measurements have been associated with changes in soils and soil map units (Hoekstra et al., 1992; Jaynes et al., 1993; Doolittle et al., 1996). For each soil, intrinsic physical and chemical properties, as well as temporal variations in soil water and temperature, establish a unique or characteristic range of apparent conductivity values.

Depth of Observation:

Considerable controversy remains concerning the depth of penetration and the use of multi-frequency conductivity meters. The theoretical penetration depth of the GEM300 sensor is dependent upon the bulk conductivity of the profiled earthen material(s) and the operating frequency of the sensor. Penetration depths are governed by the “skin-depth” effect (Won, 1980 and 1983). Skin-depth is the maximum depth of penetration for an EMI sensor operating at a particular frequency and sounding a medium of known conductivity. Penetration depth or “skin-depth” is inversely proportional to frequency (Won et al., 1996). Low frequency signals travel farther through conductive mediums than high frequency signal. Lowering the frequency will extend the depth of penetration. At a given frequency, the depth of penetration is greater in low conductivity soil than in high conductivity soils. Multifrequency sounding with the GEM300 purportedly provides the potential for multiple depths to be profiled with one pass of the sensor.

The theoretical depth of penetration or the “skin depth” can be estimated with the following formula given by McNeill (1996):

$$D = 500 / (s * f)^2 \quad [1]$$

Where s is the ground conductivity (mS/m) and f is the frequency (kHz). With the GEM300 sensor held at hip height in the vertical dipole orientation, apparent conductivity averaged 18.7, 20.4, 21.0, and 24.3 mS/m at frequencies of 3030, 6090, 9810, and 14790 Hz, respectively. Based on equation [1], the selected frequencies, and these averaged conductivities, the estimated skin depths were about 66, 45, 35, and 26 m at 3030, 6090, 9810, and 14790 Hz, respectively. While the induced magnetic fields may achieve these depths, the strengths of the response from these depths are too weak to be sensed by the GEM300 sensor. The actual depth of observation is much shallower and is defined by the depth-weighting function of the sensor and the conductivity of shallower soil horizons. As no depth-weighting functions are presently available for the GEM300 sensor, it is unclear what feature(s) or depth is providing the observed response.

Although no depth-weighting functions are available for the GEM300 sensor, measurements obtained in the horizontal dipole orientation are more sensitive to changes in apparent conductivity that occur at shallower soil depths. Measurements obtained in the vertical dipole orientation are more sensitive to changes in apparent conductivity that occurred at greater soil depths. At each frequency, the averaged measurements taken in the deeper-sensing, vertical dipole orientation were higher than those obtained in the shallower-sensing, horizontal dipole orientation. This relationship suggests the presence of more conductive layers in the subsurface than at the surface. However, apparent conductivity increased with increasing frequency. This trend may reflect differences in signal strengths at different frequencies. This is supported by the similarity in spatial patterns and the difference in signal amplitudes evident in figures 1 and 2.

Table 2 summarizes the EMI data collected with the GEM300 sensor at Juniper Bay. This inclusive data set contains all 735 measurements taken within this period of investigation. With a frequency of 3030 Hz, apparent conductivity ranged from -19.4 to 74.4 mS/m in the horizontal dipole orientation and from -48.4 to 55.7 mS/m in the vertical dipole orientation. In the horizontal dipole orientation, half of the observations had values of apparent conductivity between 8.6 and 17.9 mS/m. In the vertical dipole orientation, half of the observations had values of apparent conductivity between 11.6 and 26.1 mS/m. With a frequency of 6090 Hz, apparent conductivity ranged from -29.0 to 36.1 mS/m in the horizontal dipole orientation and from -24.1 to 49.2 mS/m in the vertical dipole orientation. In the horizontal dipole orientation, half of the observations had values of apparent conductivity between 7.3 and 18.0 mS/m. In the vertical dipole orientation, half of the observations had values of apparent conductivity between 14.7 and 27.4 mS/m. With a frequency of 9810 Hz, apparent conductivity ranged from -33.5 to 37.8 mS/m in the horizontal dipole orientation and from -27.2 to 49.6 mS/m in the vertical dipole orientation. In the horizontal dipole orientation, half of the observations had values of apparent conductivity between 6.7 and 21.2 mS/m. In the vertical dipole orientation, half of the observations had values of apparent conductivity between 13.0 and 29.6 mS/m. With a frequency of 14790 Hz, apparent conductivity ranged from -40.0 to 37.9 mS/m in the horizontal dipole orientation and from -32.6 to 51.2 mS/m in the vertical dipole orientation. In the horizontal dipole orientation, half of the observations had values of apparent conductivity between 11.3 and 24.3 mS/m. In the vertical dipole orientation, half of the observations had values of apparent conductivity between 17.1 and 33.4 mS/m.

Frequency (Hz)

	3030V(C)	3030H(C)	6090V(C)	6090H(C)	9810V(C)	9810H(C)	14790V(C)	14790H(C)
Average	18.7	12.4	20.4	11.9	21.0	12.5	24.3	16.1
SD	12.1	9.2	11.4	9.3	12.6	11.3	12.8	11.6
Minimum	-48.4	-19.4	-24.1	-29.0	-27.2	-33.5	-32.6	-40.0
Maximum	55.7	74.4	49.2	36.1	49.6	37.8	51.2	37.9
First	11.6	8.6	14.7	7.3	13.0	6.7	17.1	11.3
Second	18.1	13.3	19.8	12.9	21.7	13.6	25.3	17.9
Third	26.1	17.9	27.4	18.0	29.6	21.2	33.4	24.3

Table 2 – Basic Statistics for the EMI Survey of Juniper Bay. Values represent apparent conductivity (mS/m).

Figures 1 and 2 show the results of the EMI survey in the northwestern part of Juniper Bay. The upper and lower plots of Figures 1 show the spatial distribution of apparent conductivity recorded at frequencies of 3030 and 6090 Hz, respectively. The upper and lower plots of Figures 2 show the spatial distribution of apparent conductivity recorded at frequencies of 9810 and 14790 Hz, respectively. In each figure and for each frequency, the left-hand and right-hand plots represent data collected in the horizontal (shallower-sensing) and vertical (deeper sensing) dipole orientations, respectively. These image maps use different colors to represent the data. Colors are associated with percentage values (in relation to the minimum and maximum values). In each color plot, the isoline interval is 2 mS/m. The frequency and dipole orientation at which data were collected is shown above each plot. The depths of penetration and observation are assumed to increase as the frequency decreases. The locations of 430 observation points at which EMI data were collected are shown in the lower-left plot of Figure 2. This plot also contains the location of the detailed grid.

While measured values and spatial patterns of apparent conductivity did vary slightly with different frequencies and dipole orientations, the plots in figures 1 and 2 are remarkable similar. In general, apparent conductivity increased with increasing frequency (decreasing penetration depth). This trend was the opposite of the trend noticed in data from the December 2001 survey where conductivity decreased with increased frequency. At most observation points, apparent conductivity was higher in the deeper-sensing vertical dipole orientation than in the shallower-sensing horizontal dipole orientation.

In each plot, the survey area appears to be divided into two zones of contrasting apparent conductivity by an abrupt,

essentially east-west trending line. Apparent conductivity values are noticeably higher in the zone that is located to the south than to the north of this line. As these patterns conform to field boundaries and drainage lines, these two contrasting zones are believed to reflect differences in management. The southern 12 lines (see Figure 2, lower left-hand plot) were surveyed on 12 June while the northern 9 lines were surveyed on 14 June. During the intervening time period heavy rains from hurricane Alicia fell on the site. The increased soil moisture did not have a noticeable affect on the patterns observed in figures 1 and 2 as the conspicuous boundary occurs within the data set collected on 12 June and values of apparent conductivity are generally lower in the data collected on 14 June.

Negative apparent conductivity values help defines the boundary separating the two suspected management zones. The cause of these negative values is not known. The overhead power lines that were evident in data collected in the northwest corner of the bay during the December 2000 survey are not apparent in this data set. The present survey was conducted at a greater distance and did not encounter signal interference from these lines.

Figures 3 and 4 show the results of the EMI survey conducted within the detailed grid site (see Figure 2, lower left-hand plot for the location of the grid site) used for the preparation of three-dimensional block diagrams of the radar profiles. The upper and lower plots of Figures 3 show the spatial distribution of apparent conductivity recorded at frequencies of 6090 and 3030 Hz, respectively. The upper and lower plots of Figures 4 show the spatial distribution of apparent conductivity recorded at frequencies of 14790 and 9810 Hz, respectively. In each figure and for each frequency, the left-hand and right-hand plots represent data collected in the horizontal (shallower-sensing) and vertical (deeper sensing) dipole orientations, respectively. These image maps use different colors to represent the data. Colors are associated with percentage values (in relation to the minimum and maximum values). In each color plot, the isoline interval is 2 mS/m. The frequency and dipole orientation at which data were collected are shown above each plot.

The locations of 221 observation points at which EMI data were collected are shown in the lower-left plot of Figure 3. Data were collected along parallel rows. The converging patterns of observation points recorded with the Rockwell GPS receiver are in error. As the locations of the observation points are considered inaccurate, spatial patterns shown in these plots are also considered incorrect.

Ground-Penetrating Radar

All radar profiles have been processed through WINRAD software and converted into bitmaps. Processing was limited to signal stacking, distance normalization, color transforms, and table customizing. A CD containing the bitmap files has been forwarded with a copy of this trip report to Jared Jenkins at North Carolina State University.

During the week of July 9 through 12, 2001, I attended the Advanced Data Processing Course offered by Geophysical Survey Systems, Inc. (GSSI), in North Salem, New Hampshire. During this course, radar data from the detailed grid site were successfully processed and prepared into three-dimensional images. I am very pleased with the results. The data file for this grid was immense (over 185 megabytes). Five images of the grid site have been prepared and will be forwarded to me on a CD by GSSI. When I receive these images, I will prepare a report documenting the procedures used and discussing the results. However, as I am scheduled to be away from my office for the period of 24 July to 21 August 2001, this report cannot be filed until the latter part of August.

References:

- Daniels, D. J. 1996. Surface-Penetrating Radar. The Institute of Electrical Engineers, London, United Kingdom. 300 p.
- Doolittle, J. A. 1987. Using ground-penetrating radar to increase the quality and efficiency of soil surveys. 11-32 pp. In: Reybold, W. U. and G. W. Peterson (eds.) Soil Survey Techniques, Soil Science Society of America. Special Publication No. 20. 98 p.
- Doolittle, J., R. Murphy, G. Parks, and J. Warner. 1996. Electromagnetic induction investigations of a soil delineation in Reno County, Kansas. Soil Survey Horizons 37:11-20.

Greenhouse, J. P., and D. D. Slaine. 1983. The use of reconnaissance electromagnetic methods to map contaminant migration. *Ground Water Monitoring Review* 3(2): 47-59.

Hoekstra, P., R. Lahti, J. Hild, R. Bates, and D. Phillips. 1992. Case histories of shallow time domain electromagnetics in environmental site assessments. *Ground Water Monitoring Review*. 12(4): 110-117.

Jaynes, D. B., T. S. Colvin, J. Ambuel. 1993. Soil type and crop yield determination from ground conductivity surveys. 1993 International Meeting of American Society of Agricultural Engineers. Paper No. 933552. ASAE, St. Joseph, MI. pp. 6.

Kachanoski, R. G., E. G. Gregorich, and I. J. Van Wesenbeeck. 1988. Estimating spatial variations of soil water content using noncontacting electromagnetic inductive methods. *Can. J. Soil Sci.* 68:715-722.

McCachren, C. M. 1978. Soil Survey of Robeson County, North Carolina. USDA-Soil Conservation Service, North Carolina Agricultural Experiment Station, and Robeson County Board of Commissioners. U. S. Government Printing Office, Washington DC. 68 p.

McNeill, J. D. 1980. Electrical Conductivity of soils and rocks. Technical Note TN-5. Geonics Ltd., Mississauga, Ontario. p. 22.

McNeill, J. D. 1996. Why doesn't Geonics Limited build a multifrequency EM31 or EM38 meter? Technical Note TN-30. Geonics Limited, Mississauga, Ontario. 5 p.

Morey, R. M. 1974. Continuous subsurface profiling by impulse radar. p. 212-232. *IN: Proceedings, ASCE Engineering Foundation Conference on Subsurface Exploration for Underground Excavations and Heavy Construction, held at Henniker, New Hampshire. Aug. 11-16, 1974.*

Rhoades, J. D., P. A. Raats, and R. J. Prather. 1976. Effects of liquid-phase electrical conductivity, water content, and surface conductivity on bulk soil electrical conductivity. *Soil Sci. Soc. Am. J.* 40:651-655.

Won, I. J. 1980. A wideband electromagnetic exploration method - Some theoretical and experimental results. *Geophysics* 45:928-940

Won, I. J. 1983. A sweep-frequency electromagnetic exploration method. 39-64 pp. *IN: A. A. Fitch (editor) Development of Geophysical Exploration Methods. Elsevier Applied Science Publishers, Ltd. London.*

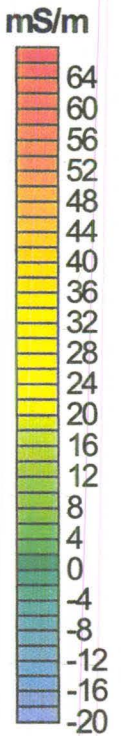
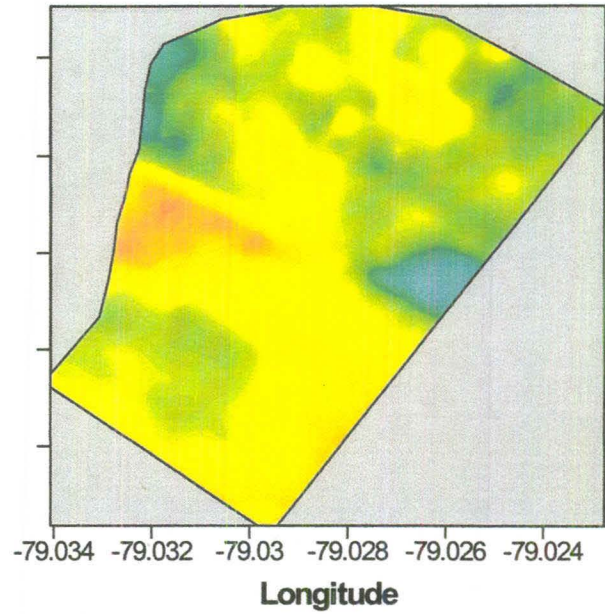
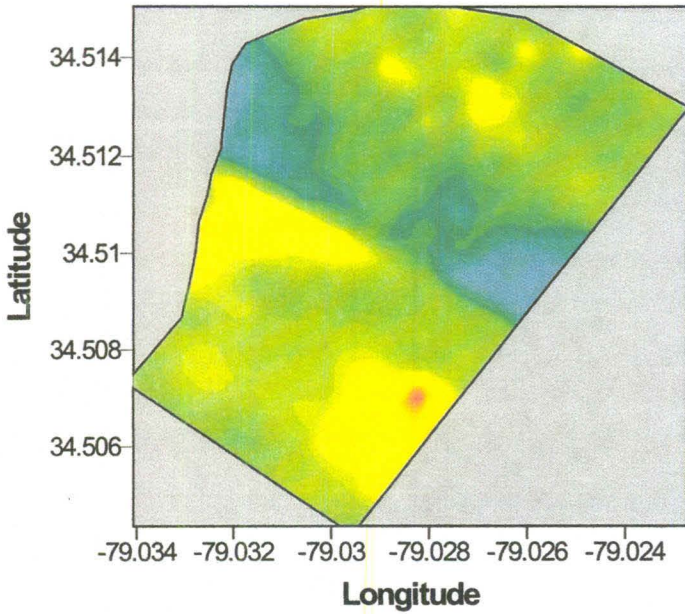
Won, I. J., Dean A. Keiswetter, George R. A. Fields, and Lynn C. Sutton. 1996. GEM-2: A new multifrequency electromagnetic sensor. *Journal of Environmental & Engineering Geophysics* 1:129-137.

EMI SURVEY JUNIPER BAY, NORTH CAROLINA GEM300 SENSOR

3030 Hz

Horizontal Dipole Orientation

Vertical Dipole Orientation



6090 Hz

Horizontal Dipole Orientation

Vertical Dipole Orientation

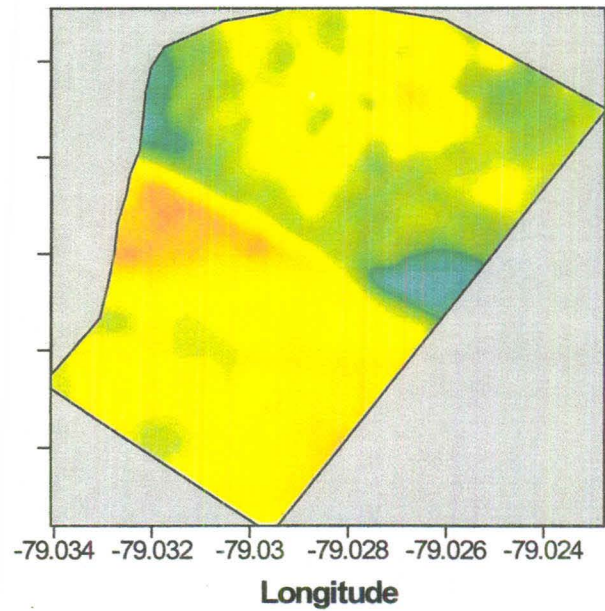
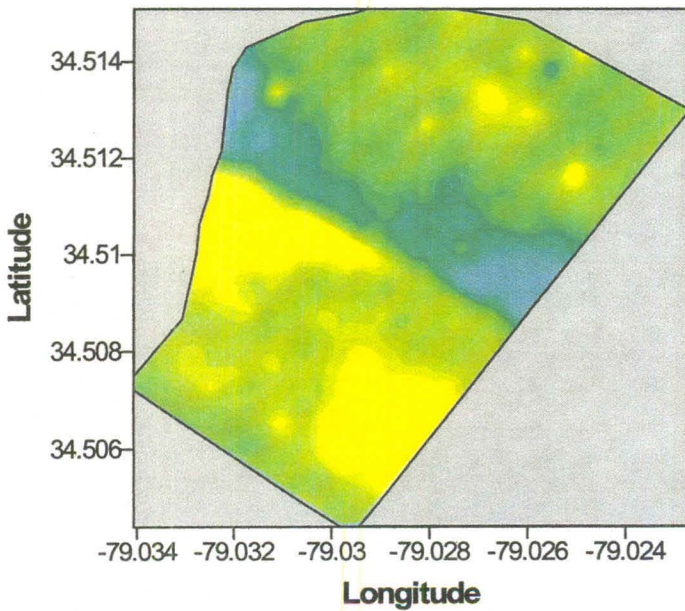


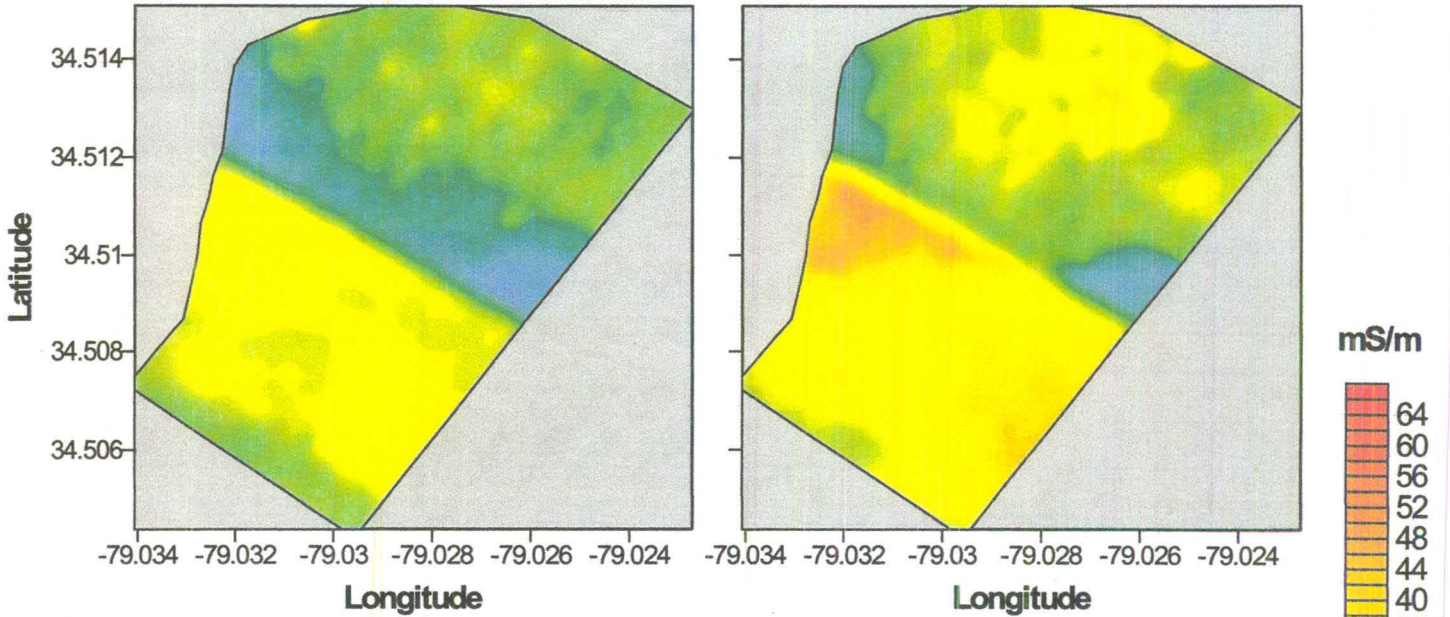
Figure 1

EMI SURVEY JUNIPER BAY, NORTH CAROLINA GEM300 SENSOR

9810 Hz

Horizontal Dipole Orientation

Vertical Dipole Orientation



14790 Hz

Horizontal Dipole Orientation

Vertical Dipole Orientation

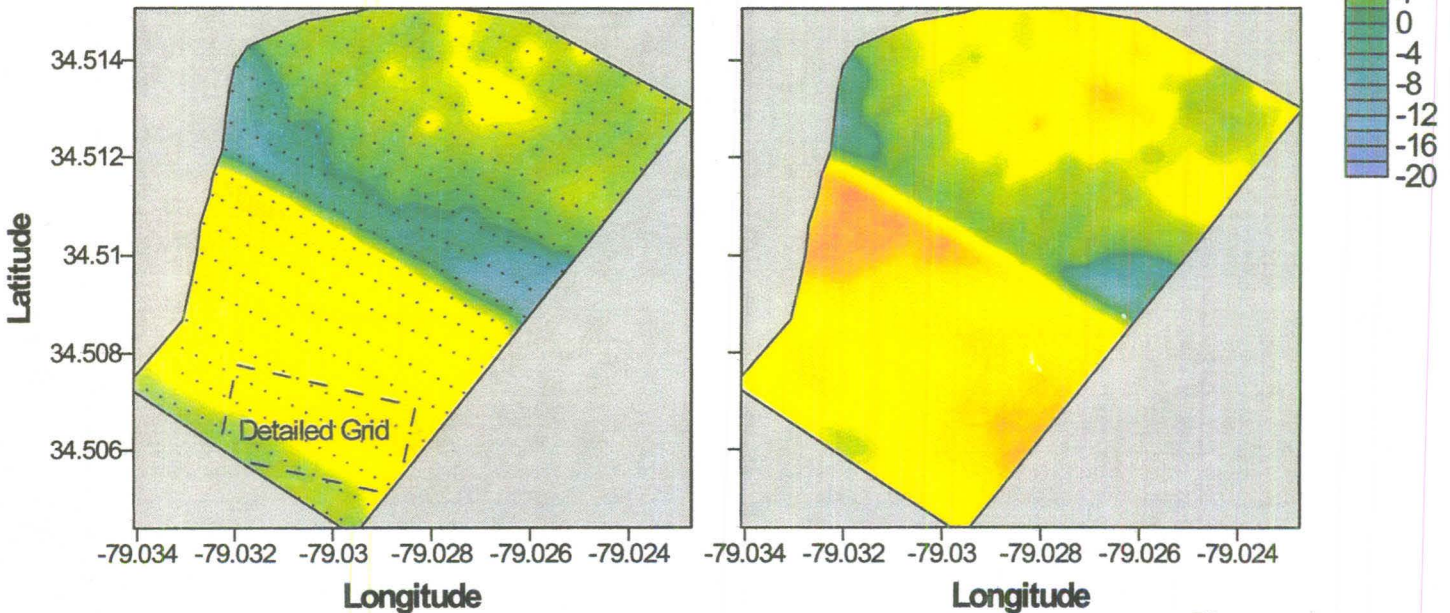


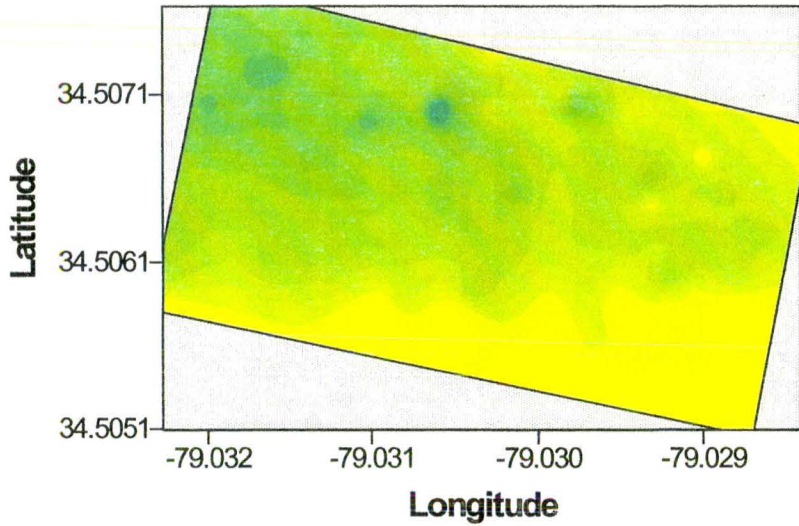
Figure 2

• Observation point

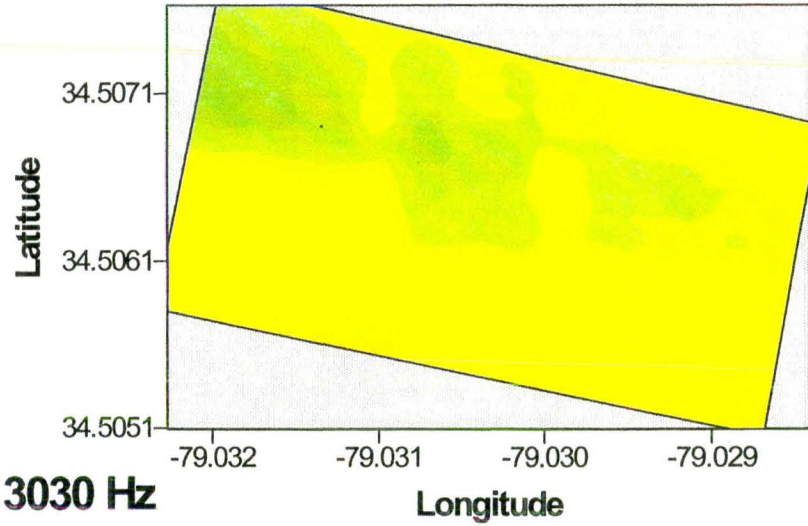
EMI SURVEY JUNIPER BAY, NORTH CAROLINA GEM300 SENSOR

6090 Hz

Horizontal Dipole Orientation

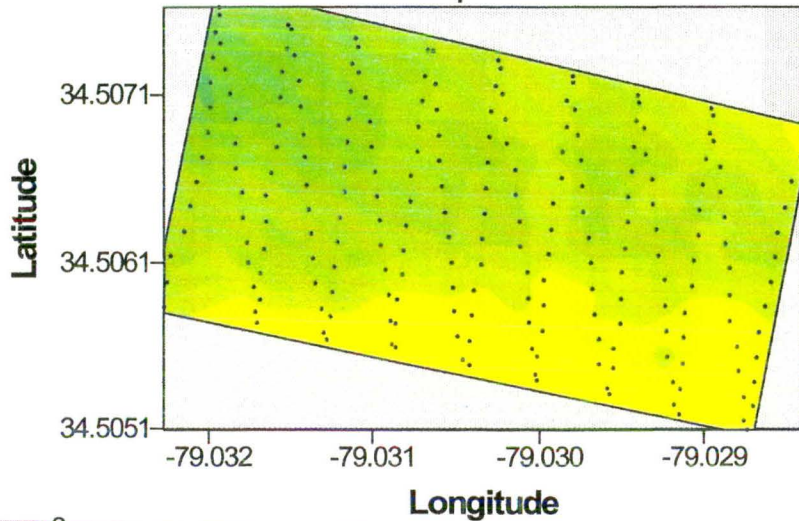


Vertical Dipole Orientation

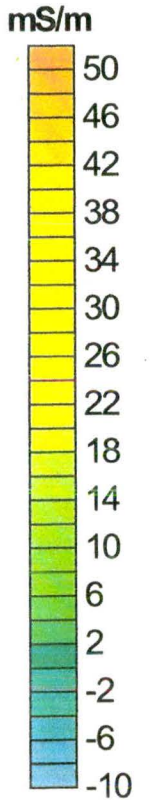
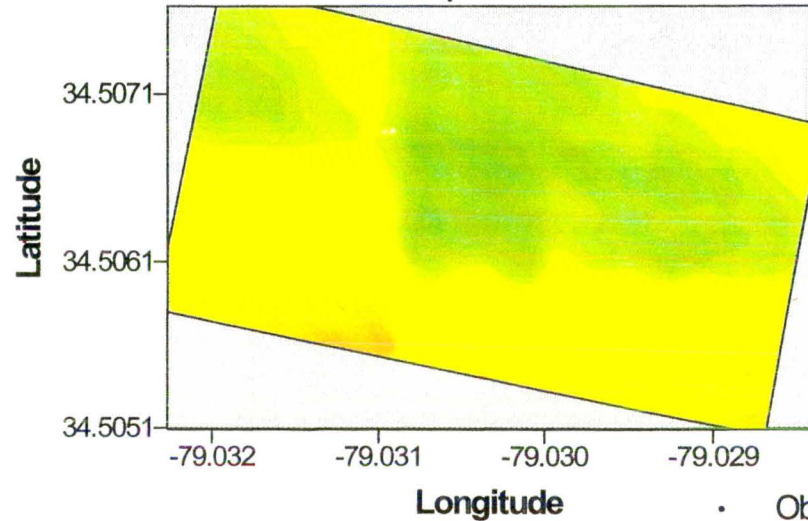


3030 Hz

Horizontal Dipole Orientation



Vertical Dipole Orientation



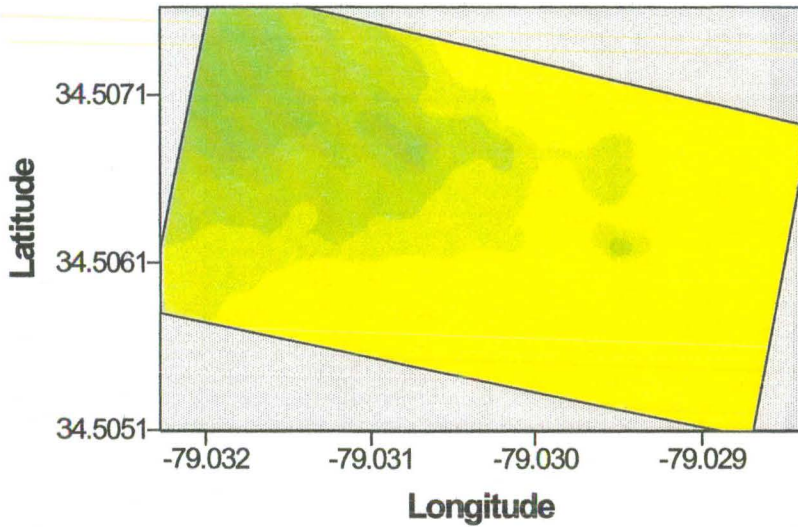
• Observation point

Figure 3

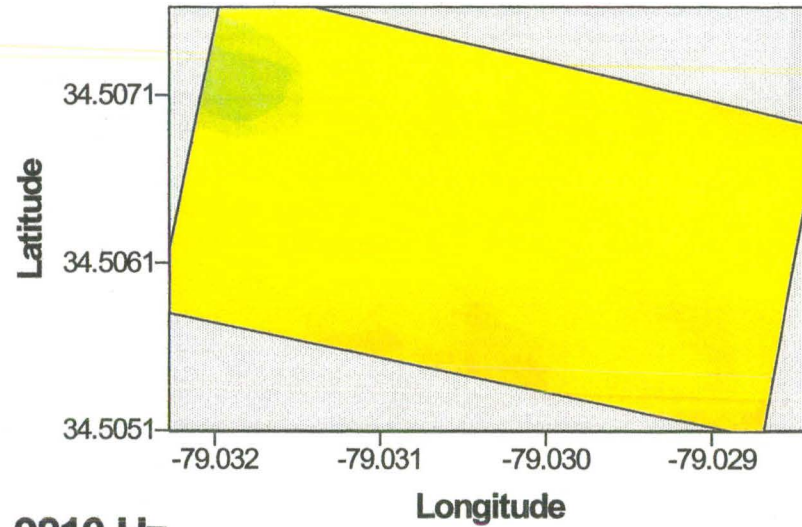
EMI SURVEY JUNIPER BAY, NORTH CAROLINA GEM300 SENSOR

14790 Hz

Horizontal Dipole Orientation

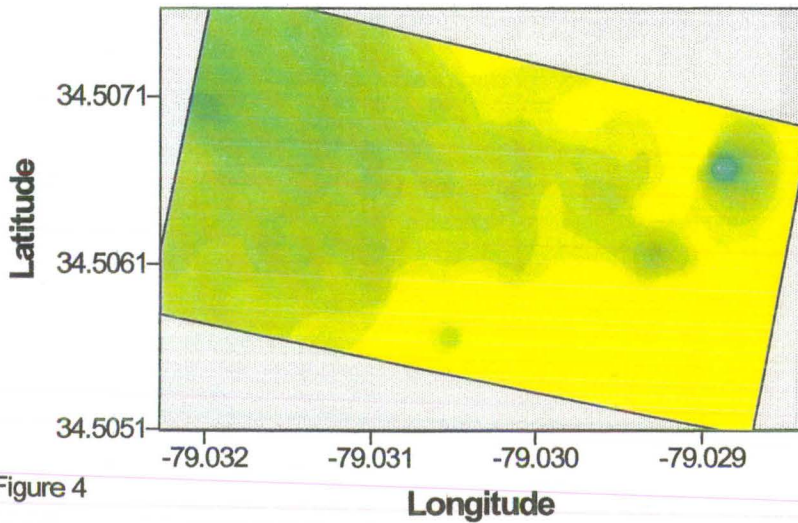


Vertical Dipole Orientation



9810 Hz

Horizontal Dipole Orientation



Vertical Dipole Orientation

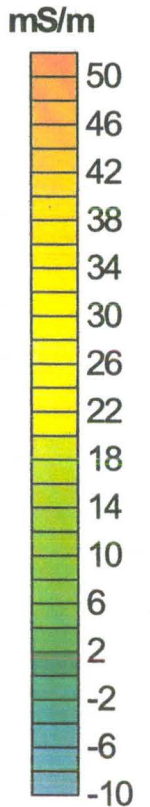
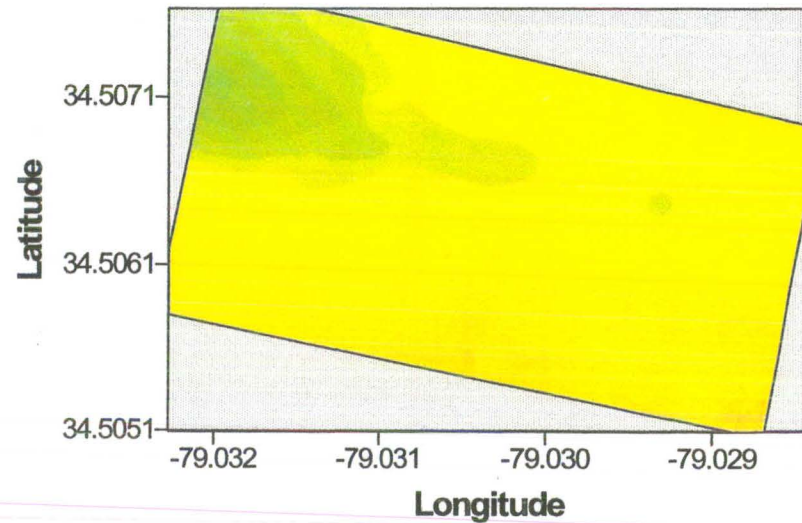


Figure 4